

## **Wind Distribution Over Beach/Dune Surface: Improving Aeolian Sand Transport Estimation**

Authors: Gomes, Nuno, Domingos, José, Jardim, Nuno, and Santos, Ricardo

Source: Journal of Coastal Research, 36(sp1) : 317-324

Published By: Coastal Education and Research Foundation

URL: <https://doi.org/10.2112/1551-5036-36.sp1.317>

---

BioOne Complete ([complete.BioOne.org](https://complete.BioOne.org)) is a full-text database of 200 subscribed and open-access titles in the biological, ecological, and environmental sciences published by nonprofit societies, associations, museums, institutions, and presses.

Your use of this PDF, the BioOne Complete website, and all posted and associated content indicates your acceptance of BioOne's Terms of Use, available at [www.bioone.org/terms-of-use](https://www.bioone.org/terms-of-use).

Usage of BioOne Complete content is strictly limited to personal, educational, and non - commercial use. Commercial inquiries or rights and permissions requests should be directed to the individual publisher as copyright holder.

---

BioOne sees sustainable scholarly publishing as an inherently collaborative enterprise connecting authors, nonprofit publishers, academic institutions, research libraries, and research funders in the common goal of maximizing access to critical research.

# Wind Distribution Over Beach/Dune Surface: Improving Aeolian Sand Transport Estimation

Nuno Gomes<sup>†</sup>, José Domingos<sup>‡</sup>, Nuno Jardim<sup>†</sup>, and Ricardo Santos<sup>†</sup>

<sup>†</sup> Earth Sciences Department

UnI-Universidade Independente

Av. Marechal Gomes da Costa, lote 9

1800-255 Lisboa, Portugal.

<sup>‡</sup> Industrial Eng. Department

UnI-Universidade Independente

## ABSTRACT



Aeolian sand transport estimation is extremely important to calculate for sediment budgets in beach/dune systems. However, the number and location of high frequency sampling ( $> 1\text{ Hz}$ ) devices deployed on the beach/dune systems still have some limitations, related basically to equipment budget and its integrity during high energy events.

Field experiments took place in Portugal, mainly along the SW and S coasts, over long periods (weeks to almost 2 years) on medium energy, non-dissipative beaches with 0.3 mm to 0.5 mm and moderate to well sorted quartz sand. Data provided by all monitoring devices was used to feed a well-tested flow model and shear velocity was calculated at every node of the monitored beach surfaces.

Although longshore wind events were affected little by beach morphology, cross-shore wind events on the other hand resulted in well-defined, heterogeneous shear velocity zones along the beach profile. Relative shear velocity values varied from a minimum on the berm to maximum on the beach-face to berm transition, with values of up to 500% of berm data. Model application to beach face, embryo dune and foredune zones consistently resulted in 150% to 200% of berm shear velocity values. Using the width of representative beach zones to calculate potential aeolian sand transport dramatically reduces its values to about 1% if monitoring equipment is located over the berm crest and to about 60% when sensors are positioned on the embryo dune zone. These values were consistent with actual/estimated rates obtained using different sand trapping devices. Low wind speed events activate the surface sporadically, reflecting micro-topography, with saltation inertia producing complex sand transport patterns, as is usually observed in situ. As wind speed increases, shear velocity relations over the whole surface are amplified, eventually resulting in narrow beach areas intensively activated while others rarely contribute as sediment source areas to aeolian transport

**ADDITIONAL INDEX WORDS:** *Aeolian sand transport, coastal dunes, wind modelling*

## INTRODUCTION

The use of well-calibrated sand budget models is being widely promoted as appropriate input for coastal management plans and subsequent strategy development (CARTER, 1988). Aeolian coastal sediment dynamics plays an important role in such models as it ensures the continuous refilling of embryo and foredune systems, vital elements for coastal protection against marine erosion (KONINGS, 1990).

Several experiments have been described in the literature, mostly concerning the efficiency of sand transport equations over narrow time intervals, in controlled wind tunnel environment (TSOAR, 1983) or in a prototype scenario (NORDSTROM *et al.*, 1996). Beach experiments are usually carried out in "close to theory" landscapes, where surface morphology, wind intensity and sediment

textural parameters combined with long fetch distances and macrotidal conditions override transport inhibitor factors. Long period monitoring is generally done using regional wind data and topographic surveys, due to problems of scale (DAVIDSON-ARNOTT and LAW, 1996).

Local high frequency (1 Hz) wind monitoring over long term periods, weeks to years, on contrasting environments has severe limitations related to basic equipment integrity, while synoptic data collection on several locations is usually limited by financial constraints. This necessitates the use of well tested fluid dispersion models, together with local monitoring stations, to produce useful outputs, compatible with geographic boundaries of coastal dune systems and the time scale on which local managers work at for their sites.

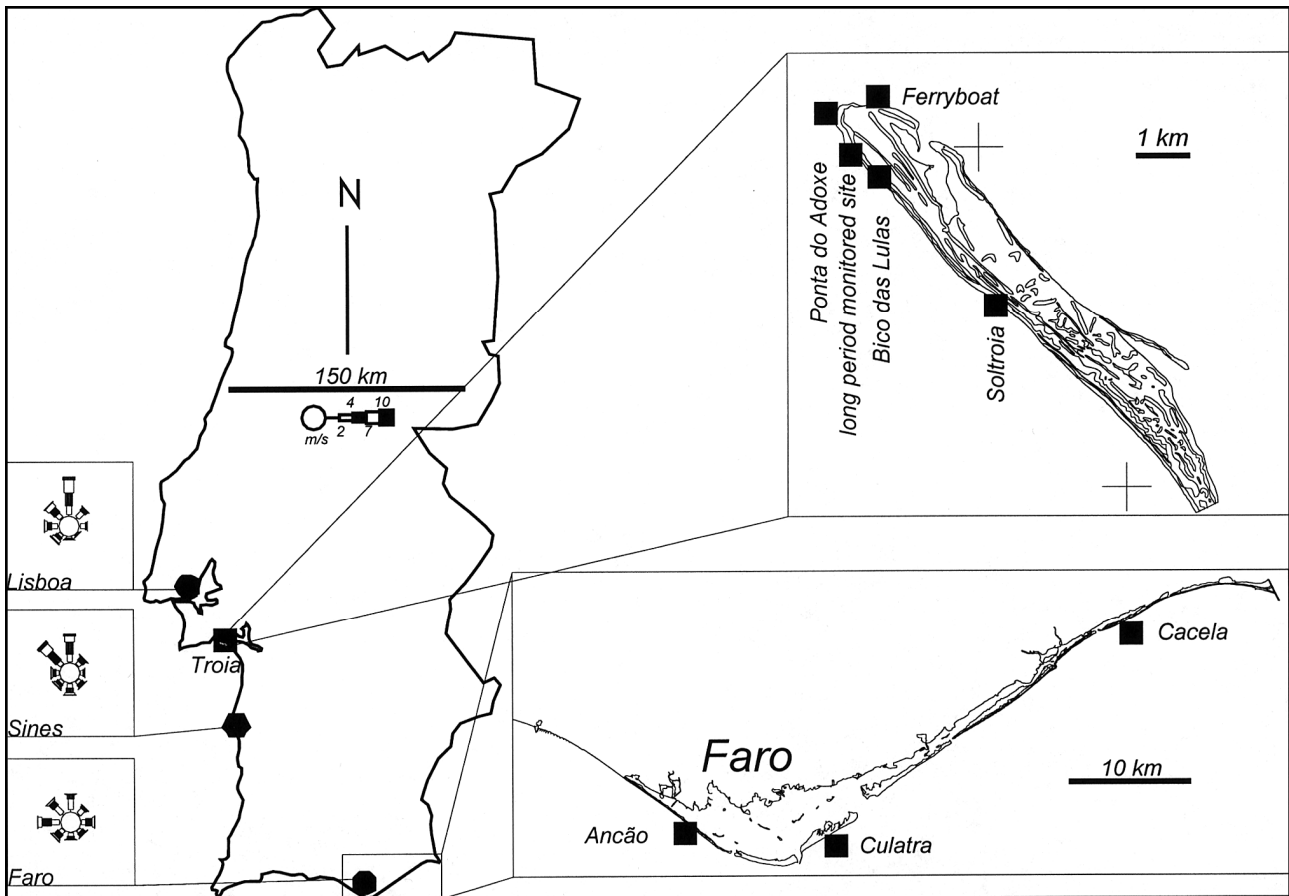


Figure 1. Schematic fieldwork site location and regional wind diagrams

A bidimensional [x,z] approach is mostly used to describe wind patterns over beach/dune systems (HSÜ, 1987; MULLIGAN, 1988) and even blowouts (FRASER *et al.*; 1998). The use of anemometer data usually integrates regional analysis, from official weather stations – generally recorded once a day, rarely at 0.5 hour average, with local readings from a limited number of sensor sets displayed vertically and recording a horizontal wind vector component at high rates ( 1 Hz).

The influence of macromorphology is well documented, particularly regarding roughness definition (SCHWIESOW and LAWRENCE, 1982) and boundary layer readjustment (JACKSON, 1977). Limitations of the use of standard linear parameters were highlighted as major factors affecting aeolian sand transport model calibration. Nevertheless the study of tri-dimensional [xyz] – cross-shore, longshore and vertical components – wind behaviour and its consequences on sand transport on natural environments is less often addressed (MIKKELSEN, 1989).

It is generally accepted that aeolian sand transport can be expressed as a function of  $u^*$ , within different levels of

complexity and indeterminacy (BAUER *et al.*, 1996). Alternatively, the use of one wind velocity reading suggested by some authors (e.g. JACKSON and McCLOSKEY, 1997), can be used when monitoring is limited to one particular system, with homogeneous roughness. The accuracy, reliability and limitations of published equations (HORIKAWA *et al.*, 1986) is not discussed in this paper and the basic, but well documented, BAGNOLD (1941) equations are often applied as a standard approach to aeolian sand transport estimation.

### METHODOLOGY

With the aim of improving the use of wind data to calculate aeolian sediment budget over natural beach/dune systems, regional wind data was analysed in order to evaluate general conditions influencing aeolian sand transport. Lisboa, Sines and Faro coastal synoptic official weather stations were used and wind data was classed in order to allow wind direction/intensity analysis (Figure 1).

## Study Area

In order to investigate the influence of beach/dune morphology on wind parameters in non-dissipative conditions, several locations were chosen in Southwestern and Southern Portugal. The selection of study areas was defined mainly according to the proximity of regional wind data, suitable beach/dune active systems, equipment security and site accessibility. Detailed beach, embryo dune and foredune microtopographic surveys were carried out in Troia Peninsula and in Ria Formosa at Culatra, Ancão and Cacela (Figure 1).

Troia Peninsula is a 20 km south-north oriented sand spit partially enclosing the Sado's river estuary, about 40 km south of Lisboa. Its development is associated with Troia-Sines sandstone cliff erosion due to Holocene sea level rise and subsequential northwards longshore drift. Coastal drift is actually less than 200,000 m<sup>3</sup> year<sup>-1</sup>, mostly captured in Sado's ebb delta, extending for about 40 km<sup>2</sup> in Troia's north edge (ANDRADE *et al*, 1998). Wave pattern analysis shows a dominant WNW direction, with stronger storms associated to SW waves.

Ria Formosa is a Holocene barrier island system covering about 60 km of the SE coast of Algarve (S Portugal), enclosing important saltmarsh areas in the vicinity of Faro. Five sandy islands, limited on both edges by Ancão peninsula (W) and Cacela peninsula (E) form the barrier system. All of the barrier system is topped with sand dunes, oriented mostly parallel to the beach. The system is asymmetrically split, with its West more narrow part facing SW, while the Eastern, wider and longer islands, face SE. Longshore drift is eastward amounting to about 150,000 m<sup>3</sup> year<sup>-1</sup> (ANDRADE, 1990), mainly fed by the erosion of the Olhos de Água where erosion of the Ancão sandstone cliffs as the main source. Wave direction is predominantly from SW, with fewer storms from SE.

## Data Acquisition

Field data collection was carried out at each site with installation of wind sensors positioned at several elevations, surface sediment sampling as well as the implementation of aeolian sand transport monitoring regimes. Equipment consisted of a number of different types of horizontal wind velocity and direction sensors, located vertically on a mast – from three to ten positions above the surface up to a height of 3m. Temperature, pressure, relative air moisture contents, total solar radiation and rain gauge sensor devices were also deployed. These sensors were complemented with at least two electronic sand traps (JACKSON, 1996) as well as one acoustic sensor developed to record saltation initiation to monitor threshold conditions. Both sets of equipment were connected to synoptic data loggers recording at 1 Hz and data was automatically downloaded on an hourly basis to a dedicated central computer using a GSM-Modem. A grid set

of 40 conventional (non-electronic) cumulative sand traps based on the LEATHERMAN (1978) design and vertical erosion/accumulation pins were used during field experiments at each site (2 weeks to almost 2 years in Troia). These were intended to monitor dispersion patterns of aeolian sand transport. All equipment and sample locations were geographically referenced.

A Tridimensional wind model was applied to local morphology, using regional wind pattern definitions – direction and intensity. Survey raw data was converted into matrix interpolated data, configuring a uniform tetrahedral node surface [x,y,z]. A segregated sequential solver algorithm was then used; where the matrix system derived from the finite element discretisation of the governing equation for each degree of freedom is solved separately. The flow problem is non-linear and the governing equations are coupled together. The sequential solution of all the governing equations constitutes a global iteration. The number of global iterations required to achieve a converged solution varies considerably, depending on the size and heterogeneity of the surface data. Using a [x,y,z] wind velocity resultant matrix, shear velocity ( $u^*$ ) is calculated at every grid point. This was accomplished using ANSYS<sup>®</sup> and a Compaq<sup>®</sup> Alpha (twin processor) and an IBM<sup>®</sup> 6000 Risk workstations running Unix.

## RESULTS

Regional predominant wind direction in Troia is N and NW. In Faro, regional wind is generally less intense, with slightly prevailing westerlies. On chosen sites, from March 1999 to September 2001, aeolian sand transport was recorded. This was more frequent in Troia and quite rare in Ria Formosa.

Mean grain size diameter for surface sediment at the sites ranged from 0.3 mm to 0.5 mm and sorting was moderate to well sorted quartz sand.

### Field wind data

Wind direction in situ, at the monitored heights rarely coincided with regional weather stations data, with terrain morphology strongly and heterogeneously affecting any possible relationship (ALCÁNTARA-CARRIÓ, 2000). This is particularly true when regional weather stations are located within urban areas.

Field wind data was analysed in order to calculate  $u^*$  and  $z^0$ . For seaward wind direction, average  $z^0$  measured values were 1.48 cm, with a maximum value of 9.5 cm, reflecting vegetation cover and foredune morphology (Figure 2). On the berm section of the beach average  $z^0$  is 0.5 mm to 1.0 mm with longshore wind, and up to 2.4mm with cross-shore wind. On the transition between the berm and beach face  $z^0$  values are from 0.1 mm to 1.0 mm with longshore wind and from 0.6 mm to 1.3 mm with cross-shore wind.

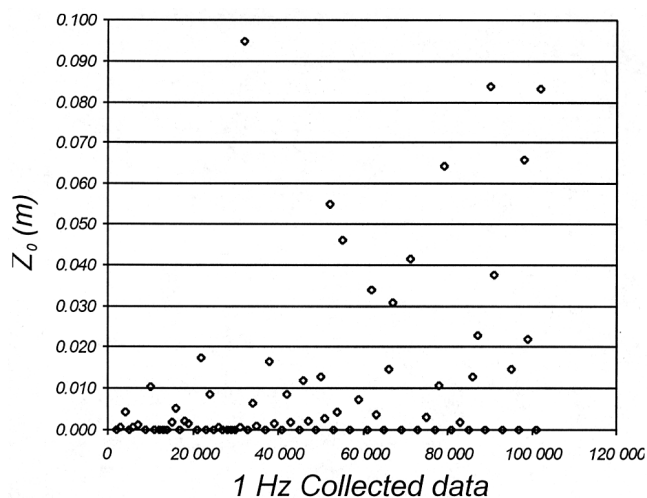


Figure 2. Roughness factor values distribution on collected data

For longshore wind events measured  $u^*$  is consistent with expected values – from null to close to  $1 \text{ ms}^{-1}$  (Figure 3). Turbulence is fully achieved and the horizontal component  $V_h[xy]$  of wind velocity plotted against  $\ln(\text{sensor height})$  follows a straight line (BAUER, 1992). For cross-shore wind, beach and foredune morphology force almost continuous boundary layer readjustments and  $u^*$  must be calculated using only close to surface sensors i.e. those located inside the boundary layer.

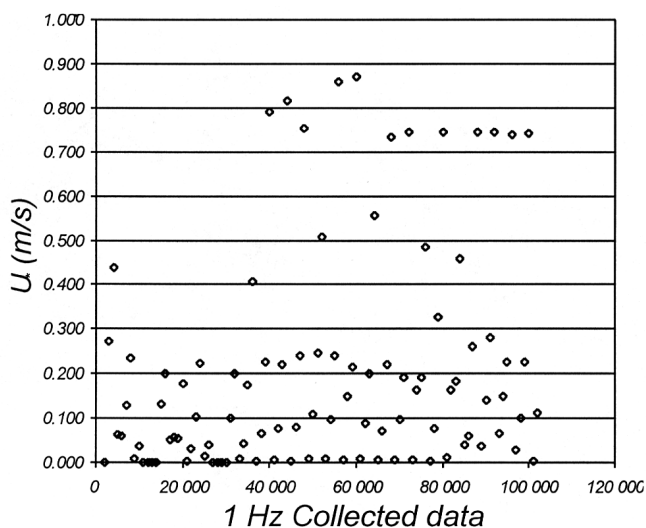


Figure 3. Shear velocity values distribution on collected data

### Sand Traps

The efficiency of high frequency sand traps varies tremendously, depending on wind intensity, sediment moisture contents and grain size (BENNETT and OLYPHANT, 1998). There were, however, enough events recorded to test a 1 Hz aeolian sand transport model. Figure 4 is an example of estimated transport values corrections, with model results reducing the scale error and improving shape adjustment. Cumulative conventional sand traps tend to be more useful in longer field experiments, whereas electronic devices were shown to be fragile. Conventional traps are also inexpensive and this is an important factor for the deployment of large trap arrays. Model calibration using total volumes of captured sand failed to explain if the errors were due just to a scaling problem or a model deviation pattern. Aeolian sand transport dispersion revealed complex behaviour, whose patterns interact randomly with the arrays of sampling traps. Different relationships were obtained even under similar environmental conditions (i.e. wind direction and intensity on the same beach) on different days. This occurred on time frames from seconds to minutes.. Trapped sediment was consistently showed to be 0.25 mm mean diameter and of quartz sand.

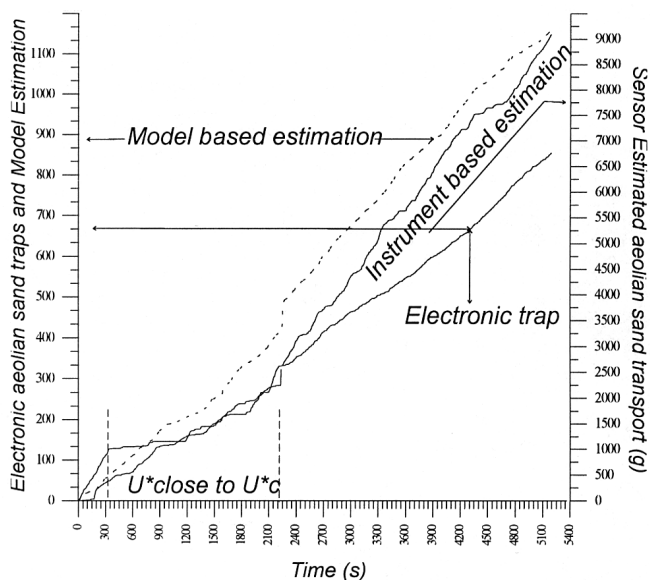


Figure 4. Estimated aeolian sand transport over the embryo dune area using  $u^*$  from the instrumented vertical array located on the beach face to berm transition., plotted against model results using obtained values for trap location and sediment trap data.

## Wind model application

Calibration of the wind/transport model results using field data was carried out using field work data sets to limit possible wind horizontal velocity ( $V_h[xy]$ ) values at a given height during the iteration process (RASMUSSEN, 1989). There are obvious limitations to the measurement system deployed due to the restricted number of wind sensors used in the vertical arrays (less than ten) as well as time scale effects. This was overcome somewhat by simplifying the process, assuming that the appropriated number of iterations at a tested height  $h$  can be applied to all of the surface. The calibration process was not applied to all sets of data ( $78.8 \times 10^6$  records) but only to selected wind activated surface events and high wind intensity events – even without aeolian sand transport.

Model node coordinates used are:  $Dx=Dy= 0.1m$  and  $Dz=0.01m$  up to  $10cm$  above the surface,  $Dz=0.05m$  from  $10cm$  to  $1.0m$  above the surface,  $Dz=0.10m$  from  $1.0m$  to  $3.0m$  and  $Dz=0.5m$  above  $h=3.0m$ .

$V_h[xy]$  results were plotted against measured values (Figure 5). As only one vertical sensor array at each beach location was used for each site model calibration, values from all sensors at every different position on the beach, for each site used, were plotted to check data fits.

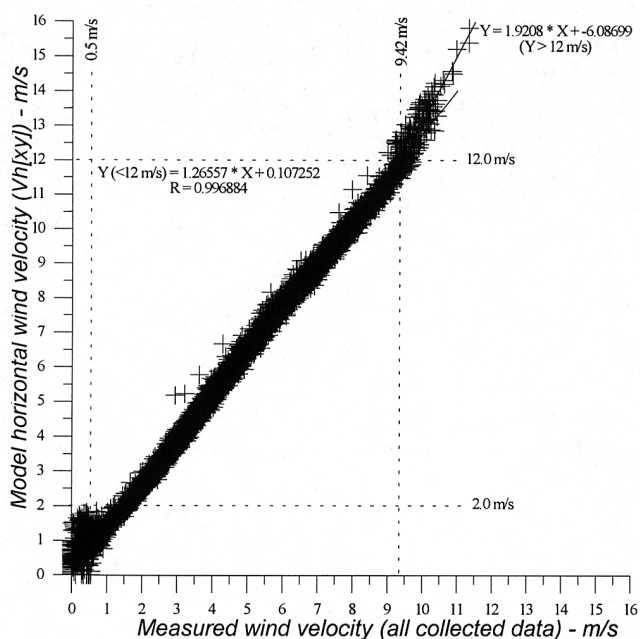


Figure 5. Measured and model wind velocity for all collected data.

Model wind velocity horizontal components were higher than measured ones, with linear regression fit,  $R_2 = 0.997$  ( $V_h[xy]_{model} = 1.266 V_h[xy]_{measured} + 0.1073$ ). When measured wind velocity is less than  $0.5 \text{ ms}^{-1}$  this is not true, and model results exceed by a factor of 2 measured values for some time. This is probably a result of sensor inaccuracy at low wind velocity levels and does not influence sand transport results, which is always related to higher wind intensity (even at lower sensors elevations). At values exceeding  $V_h[xy]_{model}=12.0 \text{ ms}^{-1}$  the relationship varies, and model results almost double field records. This can be explained both as a problem with the sensors or, more likely, as a direct result of the saltation layer roughness forcing a general wind velocity decrease. In fact, in situ conditions regarding these – somewhat rare – occasions were reported as exceptional.

It seems that most situations are conveniently described by the former equation, with all others reflecting difficulties on mathematically modelling real conditions, with variables not fully defined, or even not considered, acting as a wind velocity reduction factor. A major output in using a model of this type is the possibility of obtaining wind velocity at every height and  $u^*$  values for all points of the surface area in question, therefore the study is not just restricted to using those heights that the sensors were positioned at. Output includes the vertical wind velocity component  $V_h[z]$  (examples are shown for different beach zones in tables 1-4)

While longshore wind directions tend to result in homogeneous  $u^*$  values, cross-shore wind data produce model  $u^*$  results that varies over the studied surfaces reflecting beach/dune morphology across the typical beach face/berm with a maximum being reached at the berm crest (up to five times of the former zone). Beach face zones resulted in values 1.5 to 2.0 times that of the berm results. However, wet beach face width at high tide varies for example  $11.5m - 23.0m$  for  $10^\circ$  beach slope and  $38.2m - 76.4m$  for  $3^\circ$  beach slope. Field observations allowed the definition of 40 minutes to 70 minutes as a surface drying time interval on a sunny day.

Values obtained for dune areas (embryo and foredune) did not consider vegetation roughness factors, densities and heights (BRESSOLIER and THOMAS, 1977; WASSON and NANNINGA, 1986)

## Sand transport equations application

The use of the model  $u^*$ , filtered with threshold values ( $u^*c$ ) and calculated for a specific sediment, resulted in shape-fitted estimations. These were amplified up to 10 times for cross-shore wind direction, in cases where  $u^*$  values were slightly higher than  $u^*c$ . This is probably caused by unmonitored inertia, maintaining sand grains in saltation even when  $u^* < u^*c$ . (NICKLING, 1988;

BARNDORFF-NIELSEN, 1986 and McEWAN *et al*, 1992) Also  $u^*c$  values obtained with saltation sensors in situ were not consistent with those calculated using sediment mean diameter ( $d$ ), being systematically higher. This is probably related to surface sediment water contents (BELLY, 1964) even if there are some reported events where wet sand was activated by extreme wind events – 30 ms<sup>-1</sup> at 1m height (DRAGA, 1983). Other unmonitored inhibitor factors, such as salt contents (KROON and HOEKSTRA, 1990), shell fragments over the surface and grain shape, are a possible reason for overestimated rates of aeolian sand transport.

**DISCUSSION**

Limitations were in the study were due to inaccurate or lack of field data to feed the wind model. Surface roughness ( $z_0$ ) was considered constant for each beach zone and wave action generating ocean surface roughness was not inputted, with no considered interference between the fluid and the water. It is not possible, yet, for any surface interaction feedback to be addressed within the used model, as experimented in coarser model runs (CASTRO, 1995). Morphology was fixed for every site, as was subsequent wind analysis. Averaged values were used for air density and viscosity.

Table 1. Wind velocity values at Beach Face (distance to HTWM = 3m)

| NODE | Z (m) | h (cm) | Vh(xyz) m/s | Vh[xy] frac. | Vh[z] frac. |
|------|-------|--------|-------------|--------------|-------------|
| 6849 | 2.01  | 0.00   | 0.00        | 0.000        | 0.000       |
| 6850 | 2.11  | 10.65  | 3.15        | 0.959        | 0.284       |
| 6851 | 2.22  | 21.50  | 3.28        | 0.960        | 0.279       |
| 6852 | 2.33  | 32.57  | 3.43        | 0.962        | 0.272       |
| 6853 | 2.45  | 43.85  | 3.58        | 0.964        | 0.267       |
| 6854 | 2.56  | 55.35  | 3.71        | 0.965        | 0.262       |
| 6855 | 2.68  | 67.08  | 3.81        | 0.966        | 0.257       |
| 6856 | 2.80  | 79.04  | 3.88        | 0.968        | 0.252       |
| 6857 | 2.92  | 91.22  | 3.91        | 0.969        | 0.248       |
| 6858 | 3.04  | 103.65 | 3.93        | 0.970        | 0.243       |
| 6859 | 3.17  | 116.32 | 3.94        | 0.971        | 0.238       |
| 6860 | 3.30  | 129.24 | 3.94        | 0.972        | 0.233       |
| 6861 | 3.43  | 142.41 | 3.95        | 0.974        | 0.228       |

Table 3. Wind velocity values at Berm (distance to HTWM = 55m)

| NODE  | Z (m) | h (cm) | Vh(xyz) m/s | Vh[xy] frac. | Vh[z] frac. |
|-------|-------|--------|-------------|--------------|-------------|
| 6426  | 6.79  | 0.00   | 0.00        | 0.000        | 0.000       |
| 14107 | 6.88  | 9.18   | 3.60        | 0.993        | 0.118       |
| 14108 | 6.97  | 18.54  | 3.86        | 0.994        | 0.109       |
| 14109 | 7.07  | 28.08  | 4.07        | 0.995        | 0.102       |
| 14110 | 7.17  | 37.81  | 4.24        | 0.995        | 0.096       |
| 14111 | 7.27  | 47.73  | 4.39        | 0.996        | 0.091       |
| 14112 | 7.37  | 57.85  | 4.51        | 0.996        | 0.087       |
| 14113 | 7.47  | 68.16  | 4.61        | 0.997        | 0.083       |
| 14114 | 7.58  | 78.67  | 4.69        | 0.997        | 0.079       |
| 14115 | 7.68  | 89.39  | 4.73        | 0.997        | 0.076       |
| 14116 | 7.79  | 100.32 | 4.76        | 0.997        | 0.073       |
| 14117 | 7.90  | 111.46 | 4.77        | 0.997        | 0.071       |
| 14118 | 8.02  | 122.82 | 4.78        | 0.998        | 0.068       |
| 14119 | 8.13  | 134.40 | 4.78        | 0.998        | 0.066       |
| 14120 | 8.25  | 146.20 | 4.77        | 0.998        | 0.064       |

Table 2. Wind velocity values at Berm Crest (distance to HTWM = 6.5m)

| NODE | Z (m) | h (cm) | Vh(xyz) m/s | Vh[xy] frac. | Vh[z] frac. |
|------|-------|--------|-------------|--------------|-------------|
| 6483 | 2.84  | 0.00   | 0.00        | 0.000        | 0.000       |
| 7324 | 2.94  | 10.02  | 4.19        | 0.979        | 0.202       |
| 7325 | 3.04  | 20.23  | 4.27        | 0.980        | 0.198       |
| 7326 | 3.14  | 30.65  | 4.32        | 0.981        | 0.195       |
| 7327 | 3.25  | 41.27  | 4.39        | 0.981        | 0.192       |
| 7328 | 3.36  | 52.10  | 4.46        | 0.982        | 0.190       |
| 7329 | 3.47  | 63.14  | 4.52        | 0.982        | 0.188       |
| 7330 | 3.58  | 74.39  | 4.56        | 0.983        | 0.185       |
| 7331 | 3.69  | 85.87  | 4.57        | 0.983        | 0.183       |
| 7332 | 3.81  | 97.57  | 4.55        | 0.984        | 0.181       |
| 7333 | 3.93  | 109.49 | 4.53        | 0.984        | 0.178       |
| 7334 | 4.05  | 121.65 | 4.51        | 0.984        | 0.176       |
| 7335 | 4.18  | 134.05 | 4.48        | 0.985        | 0.173       |
| 7336 | 4.30  | 146.69 | 4.46        | 0.985        | 0.171       |
| 7337 | 4.43  | 159.58 | 4.44        | 0.986        | 0.168       |

Table 4. Wind velocity values at Embryo dune (distance to HTWM = 83m)

| NODE  | Z (m) | h (cm) | Vh(xyz) m/s | Vh[xy] frac. | Vh[z] frac. |
|-------|-------|--------|-------------|--------------|-------------|
| 6393  | 8.29  | 0.00   | 0.00        | 0.000        | 0.000       |
| 18034 | 8.38  | 8.86   | 3.99        | 0.995        | 0.100       |
| 18035 | 8.47  | 17.90  | 4.27        | 0.995        | 0.096       |
| 18036 | 8.56  | 27.11  | 4.46        | 0.996        | 0.091       |
| 18037 | 8.65  | 36.50  | 4.60        | 0.996        | 0.087       |
| 18038 | 8.75  | 46.08  | 4.73        | 0.996        | 0.084       |
| 18039 | 8.85  | 55.84  | 4.85        | 0.997        | 0.082       |
| 18040 | 8.95  | 65.79  | 4.96        | 0.997        | 0.079       |
| 18041 | 9.05  | 75.94  | 5.05        | 0.997        | 0.077       |
| 18042 | 9.15  | 86.29  | 5.12        | 0.997        | 0.075       |
| 18043 | 9.26  | 96.84  | 5.15        | 0.997        | 0.074       |
| 18044 | 9.36  | 107.59 | 5.16        | 0.997        | 0.072       |
| 18045 | 9.47  | 118.56 | 5.16        | 0.998        | 0.071       |
| 18046 | 9.58  | 129.74 | 5.15        | 0.998        | 0.069       |
| 18047 | 9.70  | 141.14 | 5.14        | 0.998        | 0.068       |

When more than one monitor array was used, wind velocity related time interval was not used when calibrating model values for both locations [1 and 2]. It was assumed that at a given moment  $V_h[x_2y_2]$  was different and independent from  $V_h[x_1y_1]$ .

When measuring close to surface wind properties, using any equipment, interaction with the sensor and support structures caused turbulence. For long period beach monitoring, errors occur when wind direction causes the flow to adjust to local obstacles, creating a shadow zone in the sensor vicinity.

## CONCLUSIONS

Using model wind values to calculate potential sand transport in the beach/embryo dune system results in about 1% of that obtained using extrapolated sensor data located on the berm crest. If the equipment is deployed over the back beach or unvegetated embryo dune,  $u^*$  is reduced to around 60%. Values obtained are consistent with sand transport rates measured at different time intervals and with sand traps (GOMES *et al.*, 1994), tracers (BERG, 1983) or topographic surveys (GOMES *et al.*, 1992) at different locations. This clearly suggests that the use of a tri-dimensional wind model approach to answer planners and managers pertinent questions for managing these sites is valid.

Other uncontrolled environmental inhibiting factors play an important role in aeolian transport, particularly at levels close to threshold conditions, resulting in raised  $u^*c$  values. In these situations, the surface can be sporadically activated by gusts (LEE, 1987) and saltation inertia produces complex and erratic sand transport patterns. As wind speed increases, area definition is clarified with  $u^*$  exceeding  $u^*c$  on the beach face and over the berm crest (a major aeolian sand transport source area). This however, does not apply at or up until an hour after high tide.

Each beach has a different aeolian sand transport potential, depending on local beach/dune morphology, wind patterns, and surface characteristics (sediment texture, moisture contents and roughness factors). It is highly recommended that local data is used to calibrate wind models in order to calculate shear velocity ( $u^*$ ) for each site. Use of Bagnold's widely applied formulations produced good results, with both measured and calculated wind velocity values.

## ACKNOWLEDGEMENTS

This work was made possible under the framework of IMAR – Institute for Marine Research, as part of Imoarea SA Environmental Impact Assessment, carried out in Troia, under the coordination of Prof. F. Andrade and in Ria Formosa as part of FCT funded project CROP – Cross-Shore Processes on Contrasting Environments, (PDCTM/P/MAR/ 15265/ 1999), under the coordination of Prof. A. Dias.

The authors gratefully acknowledge Eng. R. Cunha, M. Carapu o. N. Morgado, N. Mira, T. Sameiro and J. Garcia for their helpful assistance with electronics, laboratory techniques and with fieldwork.

A special mention also to Prof. C. Andrade, Dr. A. Cooper and Dr. D. Jackson for their support, discussion, equipment and recollections.

## LITERATURE CITED

- ALCÁNTARA-CARRIÓ, J., ALONSO, I. 2000. Aeolian sand transport across the Isthmus of Jandia (Fuerteventura): An annual rates prediction. *Actas do Simpósio Brasileiro sobre praias arenosas*, 70-72.
- ANDRADE, C. 1990. *O ambiente de barreira da Ria Formosa. Algarve - Portugal*. PhD Thesis. Univ. Lisboa. (in portuguese). 643 pp.
- ANDRADE, F., BAPTISTA R., FERREIRA A., GOMES N., MELO J.J., LEITÃO P., PINTO M.J. 1998. *Estudo Ambiental Estratégico para a Península de Tróia*. Int.Rep. 1-2. (in Portuguese). 38pp.
- BAGNOLD, R. A. 1941. *The physics of blown sand and desert dunes*. Morrow, New York, 265 pp.
- BARNDORFF-NIELSEN, O.E. 1986. Sand, wind and statistics: Some recent investigations. *Acta Mechanica* 64, 1-18.
- BAUER, B. O., DAVIDSON – ARNOTT, R. G. D., NORDSTROM, K.F., OLLERHEAD, J., JACKSON, N.L. 1996. Indeterminacy in aeolian sediment transport across beaches. *Journal of Coastal Research*, 12(3) 641-653.
- BAUER, B.O., SHERMAN, D.J. WOLCOTT, J.F. 1992. Sources of uncertainty in shear stress and roughness length estimates derived from velocity profiles. *Professional Geographer*, 44(4), 453-464
- BELLY, P.Y. 1964. *Sand movement by wind*. U.S. Army Coastal Eng. Research Center, Tech.Memorandum 1, 38 pp.
- BENNETT, S.W., OLYPHANT, G.A. 1998. Temporal and spatial variability in rates of eolian transport determined from automated sand traps: Indiana dunes National Lakeshore, U.S.A., *Journal of Coastal Research*, 14(1), 283-290.



- BERG, N.H. 1983. Field Evaluation of some sand transport models. *Earth Surface Processes and Landforms*, Vol.8, 101-114.
- BRESSOLIER, C. and THOMAS, Y.F. 1977. Studies on wind and plant interactions on French Atlantic coastal dunes. *Journal of Sedimentary Petrology*, Vol.47, No.1, 331-338.
- CARTER, R.W.G. 1988. *Coastal Environments*. Academic Press, 617 pp.
- CASTRO, F. 1995. Computer simulation of the dynamics of a dune system. *Ecological Modelling* 78, 205-217.
- DAVIDSON-ARNOTT, R.G.D. and LAW, M.N. 1996. Measurement and prediction of long term sediment supply to coastal foredunes. *Journal of Coastal Research*, 12(3), 654-663.
- DRAGA, M. 1983. Eolian activity as a consequence of beach nourishment – observations at Westerland (Sylt), German North Sea coast. *Zeitschrift für Geomorphologie* N.F.-Bd 45 303-319.
- FRASER, G.S., BENNETT, S.W., OLYPHANT, G.A., BAUCH, N.J., FERGUSON, V., GELLASCH, C.A., MILLARD, C.L., MUELLER, B., O'MALLEY, P.J., WAY, J.N. WOODFIELD, M.C. 1998. Windflow circulation patterns in a coastal dune blowout, South Coast of Lake Michigan. *Journal of Coastal Research*, 14(2), 451-460.
- GOMES, N., ANDRADE, C., NEVIN, G., MCCLOSKEY, J., JACKSON, D. 1994. Aeolian sand transport in Culatra barrier, Ria Formosa (Portugal). *Proc. Littoral 94*, ed. Eurocoast, 509-516.
- GOMES, N., ANDRADE, C., ROMARIZ, C. 1992 Sand transport rates in the Tróia-Sines arc, S.W. Portugal. In: *Coastal Dunes*, R.W.G. Carter, T.G.F. Curtis, M.J. SHEELY-SKEFFINGTON (eds.) - Balkema (Rotterdam), 33-42.
- HORIKAWA, K., HOTTA, S., KRAUS, N.C. 1986. Literature review of sand transport by wind on a dry sand surface. *Coastal Engineering*, 9, 503-526.
- HSÜ, S.A. 1987. Air flow over dunes. *Coastal Sediments*, '87, 188-201.
- JACKSON, D.W.T. 1996. A new, instantaneous aeolian sand trap design for field use. *Sedimentology* 43, 791-796.
- JACKSON, D.W.T. and McCLOSKEY, J. 1997. Preliminary results from a field investigation of aeolian sand transport using high resolution wind and transport measurements. *Geophysical Research Letters*, Vol.24, No.2, 163-166.
- JACKSON, P.S. 1977. Aspects of surface wind behaviour. *Wind Engineering*, Vol.1, N.1, 1-14.
- KONINGS, Ph. 1990. Eolian sand transport at the Belgian coast: morphodynamic implications and use in coastal management. *Proc. Littoral 90, Marseille*, Eurocoast, 120-124
- KROON, A. and HOEKSTRA, P. 1990. Eolian sediment transport on a natural beach. *Journal of Coastal Research*, 6(2), 367-379
- LEATHERMAN, S.P. 1978. A new aeolian sand trap design. *Sedimentology* 25, 303-306.
- LEE, J.A. 1987. A field experiment on the role of small scale wind gustiness in aeolian sand transport. *Earth Surface Processes and Landforms*, Vol.12, 331-335.
- McEWAN, I.K., WILLETTS, B.B., RICE, M.A. 1992. The grain/bed collision in sand transport by wind. *Sedimentology* 39, 971-981.
- MIKKELSEN, H.E. 1989. Wind flow and sediment transport over a low coastal dune. *Geoskrifter* 32, Geologisk Institut Aarhus Universitet, 46 pp.
- MULLIGAN, K.R. 1988. Velocity profiles measured on the windward slope of a transverse dune. *Earth Surface Processes and Landforms*, Vol.13, 573-582.
- NICKLING, W.G. 1988. The initiation of particle movement by wind. *Sedimentology*, 35, 499-511
- NORDSTROM, K.F., BAUER, B.O., DAVIDSON-ARNOTT, R.G.D., GARES, P.A., CARTER, R.W.G., JACKSON, D.W.T., SHERMAN, D.J. 1996. Offshore aeolian transport across a beach: Carrick Finn Strand, Ireland, *Journal of Coastal Research*, 12(3), 664-672.
- RASMUSSEN, K.R. 1989. Some aspects of flow over coastal dunes. *Proceedings of the Royal Society of Edinburgh*, 96B, 129-147.
- SCHWIESOW, R.L., LAWRENCE, R.S. 1982. Effects of a change of terrain height and roughness on a wind profile. *Boundary Layer Meteorology* 22, 109-122.
- TSOAR, H. 1983. Wind tunnel modelling of echo and climbing dunes. *Developments in Sedimentology*, 38, 247-259.
- WASSON, R.J. and NANNINGA, P.M. 1986. Estimating wind transport of sand on vegetated surfaces. *Earth Surface Processes and Landforms*, Vol.11, 505-514